Optimization Based Tuning of Autopilot Gains for a Fixed Wing UAV

Mansoor Ahsan, Khalid Rafique, and Farrukh Mazhar

***Abstract*—**Unmanned Aerial Vehicles (UAVs) have gained tremendous importance, in both Military and Civil, during first decade of this century. In a UAV, onboard computer (autopilot) autonomously controls the flight and navigation of the aircraft. Based on the aircraft role and flight envelope, basic to complex and sophisticated controllers are used to stabilize the aircraft flight parameters. These controllers constitute the autopilot system for UAVs. The autopilot systems, most commonly, provide lateral and longitudinal control through Proportional-Integral-Derivative (PID) controllers or Phase-lead or Lag Compensators. Various techniques are commonly used to 'tune' gains of these controllers. Some techniques used are, in-flight step-by-step tuning, software-in-loop or hardware-in-loop tuning methods. Subsequently, numerous in-flight tests are required to actually 'fine-tune' these gains. However, an optimization-based tuning of these PID controllers or compensators, as presented in this paper, can greatly minimize the requirement of in-flight 'tuning' and substantially reduce the risks and cost involved in flight-testing.

***Keywords*—**Unmanned aerial vehicle (UAV), autopilot, autonomous controls, PID controler gains tuning, optimization.

I. Introduction

OVER the past few decades the huge potential of unmanned aerial vehicle (UAV) in multitude of fields has been explored; which includes surveillance, reconnaissance, telemetry, weather forecast etc. It can be stated without any doubt that all commercial as well as unmanned flight will be unmanned in near future. Today the modern aircraft rely on the onboard autopilot system. Aircraft design is a multidisciplinary problem which requires expertise in various engineering fields like propulsion, flight controls, structures, aerodynamics, and feedback control systems. A typical autopilot system generate the autonomous control commands to perform various flight operation; thereby reducing the pilot fatigue in manned aircraft and operator's work load in UAVs [1]. The autopilot design primarily relies upon the knowledge of automatic flight control system. Wherein, actuator control commands are automatically produced by autopilot specific to the aircraft mission requirement to maintain a specific flight mode. The basic operation which almost all autopilot perform is the Altitude-acquire-and-hold. This operation help aircraft maintain a given altitude catering all in flight disturbances requiring minimum pilot or operator input. A brief summary of prior work cited in literature in the field of autopilot design is given in the following paragraphs.

Alvarado et al. [2] presented a heading hold controller development for a ground vehicle. The technique employed classical PID based control. The simulations were carried out in Simulink and the experimental results validated the simulations. Høstmark in [3] described a comprehensive design methodology for modeling, simulation and control of a fixed wing surveillance UAV's flight control. The AeroSim blockset for Matlab is employed for modeling and simulation. The PID based controller was used for the model.

The control methodology for modeling and control in longitudinal axis of an underwater high speed super-cavitation vehicle is presented in [4]. Two outer loop control strategies are implemented to achieve better stability and tracking.

A detailed strategy to address guidance and control predicament for a small electric-powered Autonomous Soaring UAV is elucidated in [5]. The autonomous flight used the thermals in the lower atmosphere due to convection for energy efficient vehicle flight. Outer-loop guidance and control for soaring was incorporated in the UAV's autopilot. The aircraft position, calculated thermal size and total energy state were employed for estimating guidance commands to gain altitude and conserve energy. In another work [6], a vision based technique is presented to achieve the attitude estimation without using an angular sensor for a low cost, fixed wing UAV. Flight parameters are calculated using image processing technique, which include morphological smoothing, edge detection, Hough transform, Extended Kalman Filter and statistical techniques.

Chalamont in [7] presented the automated launch and recovery of a UAV onto a cable behind a carrier aircraft. The study presents the analysis for both with turbulence and turbulence free model for the attachment cable motion behind carrier aircraft. The study comprised capturing device selection, cable modeling to estimate the cable equilibrium position in air, UAV flight control system model for UAV approach and docking onto the carrier aircraft. The design includes classical PID based controllers for pitch attitude and altitude hold; whereas speed control of the UAV is given to achieve the vehicle approach speed.

The flight control model encompassing course stabilization, altitude control and obstacle avoidance for a miniature blimp employing biological reactive system of the brain of a fly & locust is given in [8]. The study concluded that optical input is sufficiently robust to achieve course stabilization and altitude control in an unmanned flight. Likewise, in [9] the landing strategy used by honey bees is investigated for use in automatic

Mansoor Ahsan and Farrukh Mazhar are with the National University of Sciences and Technology, H-12, Islamabad, Pakistan.

Khalid Rafique is with the College of Electrical Engineering, Purdue University, USA (e-mail: khalidrafique@gmail.com).

slow speed UAV landing. The technique employed used a constant magnitude of optical flow of ground image and constant descent angle.

Various new technologies are also being investigated for UAV for example [10] presents the image based target's location estimation for a fixed wing miniature UAV within 5m of accuracy from its GPS location. Likewise in [11] the performance of a software-enabled Receding Horizon Control (RHC) is analyzed in a fault induced environment to demonstrate advanced guidance and fault detection concepts. This technology permits reconfiguration of flight in case any fault occurs in the system to ensure reliable autonomous flight. In [12] sliding mode control technique is used to for trajectory tracking to cater various uncertainties like pressure disturbances, wind factor etc and noise. The presented methodology found to be more effective and adaptive to change than conventional PID based control.

Presently, a number of autopilots are commercially available that can be installed with minor reconfigurations on a variety of fixed wing aircraft. Most of the commercially available UAV autopilots use PID control loops and/or compensators for various control operations [13]. PID control technique is widely used due to its past record of wide availability and simplicity of use [14]. Almost all these autopilots require in-flight step-by-step, software-in-loop or hardware-in-loop manual methods to tune the gains of the said controllers.

The integration of a commercially available autopilot system for use on a commercially available UAV platform is explained in [15]. The autopilot has PID based controllers with tunable gains for achieve best controller performance. The study incorporates speed, altitude, bank angle controller for the UAV. Additionally autonomous path planning and flight plan following is also implemented for UAV.

Beard et al. [16] reported the design and implementation of a small semi-autonomous fixed-wing UAV. The study includes the integration of a small low cost autopilot into the UAV. The paper also describe real-time flight path planning, trajectory smoothing and tracking. In [17] the optimal sensor selection methodology with best suited performance for a specific autopilot system of a UAV is given. The technique employs Matlab Simulink based simulations.

The development of attitude and heading controller for a rotary wing UAV is presented in [18]. The algorithm is based upon simple multi-loop SISO proportional attitude and heading controllers. The development process of avionics system for a UAV is given in [19]. The study employed Matlab Simulink simulations, commercially available controllers, radio link etc. the paper provide a broader technological guidelines for UAV development.

In this paper, optimization based tuning of an altitude-hold phase lead compensator has been demonstrated. The altitude acquire-and-hold controller has been implemented using the nonlinear mathematical model of a fixed wing UAV in Simulink Matlab [20]. The optimization of gains of said controller has been tuned using various optimization toolboxes available in the Matlab.

II. Problem Description

A. Objective Function

The altitude acquire-and-hold controller is designed with only elevator input to change the aircraft altitude, with a fixed thrust. Simplified design of the said controller is presented in Fig. 1 as following.

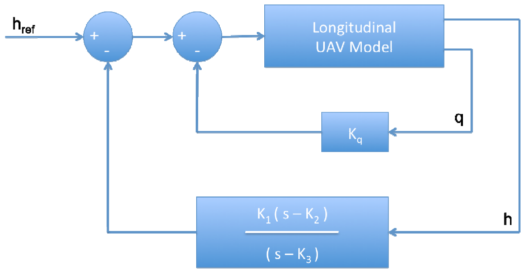

Fig. 1 Altitude-Acquire & Hold Phase Lead Compensator

As evident from the Fig. 1, our objective is to minimize the error (*e*) between the desired altitude (h_{ref}) and the plant output i.e. present altitude (*h*), as following:

$$u = \left| h_{ref} - h_{present} \right| \tag{1}$$

Present altitude and current pitch rate is used as feedback to control this error. The controller (Phase Lead Compensator) works on the present altitude and simple proportional gain is used for the pitch rate feedback. Laplace transform of this compensator in frequency domain can be written as:

$$u(s) = h_{ref} - \frac{K_1 (s - K_2)}{(s - K_3)} h(s) - K_4\, q(s) \tag{2}$$

K_4 being a simple proportional gain and easily tunable can be set manually and has been set to 20 for simplicity of the problem. Therefore, our design variables become K_1 , K_2 , and K_3.

It is important to note that *u(s)* is not our objective function. As Matlab/Simulink is used to model the problem, therefore, a time-based reference signal (y_{ref}) is specified and Simulink computes errors between this reference signal and simulated output of the plant over time, which really becomes the objective function.

The reference signal is defined as a sequence of amplitude and time pairs:

$$y_{ref}(t_{ref}), t_{ref} \in \left\{ T_{ref\,0}, T_{ref\,0}, \ldots, T_{refN} \right\} \tag{3}$$

The software computes the simulated response as a sequence of time-amplitude pairs:

$$y_{sim}(t_{sim}), t_{sim} \in \left\{ T_{sim0}, T_{sim0}, \ldots, T_{simN} \right\} \tag{4}$$

A new time base, t_{new} is formed from the union of the elements of t_{ref} and t_{sim}. Elements that are not within the minimum-maximum range of both t_{ref} and t_{sim} are omitted:

$$t_{new} = \left\{ t : t_{sim} \cap t_{ref} \right\} \tag{5}$$

Using linear interpolation, Simulink computes the values of y_{ref} and y_{sim} at the time points in t_{new} and then computes the scaled error:

$$e(t_{new}) = \frac{\left(y_{sim}(t_{new}) - y_{ref}(t_{new}) \right)}{\max\limits_{t_{new}} | y_{ref} |} \tag{6}$$

Finally, the Simulink computes the weighted, integral square error:

$$f = \int w(t) e(t)^2 \, dt \tag{7}$$

This is indeed our objective function. Here, *w(t)* is the weight vector for specifying more importance to critical responses. Default value of *1* has been used for all simulations.

For multi-objective problems, these integral errors are summed together.

$$F = \sum_{i=1}^{n} f_i \tag{8}$$

Only one objective function has been used for the purpose of this paper.

B. Constraints

Six inequality and two equality constraints define the feasible region.

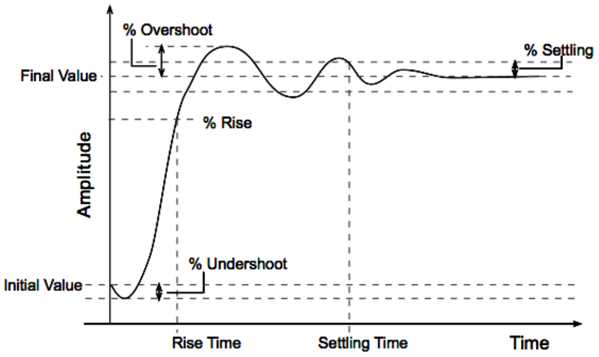

Fig. 2 Signal Constraints for a unit step input

These constraints are piecewise linear bounds. A piecewise linear bound y_{bnd} with n edges can be represented as:

$$y_{bnd}(t) = \begin{cases} y_1(t) & t_1 \le t \le t_2 \\ y_2(t) & t_2 \le t \le t_3 \\ \vdots & \vdots \\ y_n(t) & t_n \le t \le t_{n+1} \end{cases} \tag{9}$$

The software computes the signed distance between the simulated response and the edge. The signed distance for lower bounds is:

$$c = \begin{bmatrix} \max\limits_{t_1 \le t \le t_2} y_{bnd} - y_{sim} \\ \max\limits_{t_2 \le t \le t_3} y_{bnd} - y_{sim} \\ \max\limits_{t_n \le t \le t_{n+1}} y_{bnd} - y_{sim} \end{bmatrix} \tag{10}$$

where y_{sim} is the simulated response and is a function of the parameters being optimized. The signed distance for upper bounds is:

$$c = \begin{bmatrix} \max\limits_{t_1 \le t \le t_2} y_{sim} - y_{bnd} \\ \max\limits_{t_2 \le t \le t_3} y_{sim} - y_{bnd} \\ \max\limits_{t_n \le t \le t_{n+1}} y_{sim} - y_{bnd} \end{bmatrix} \tag{11}$$

All constraints above should be less than or equal to zero for a feasible solution. All constraints are automatically scaled and normalized by Simulink like Excel Solver.

C. Design Variable Bound

Similarly, appropriate bounds on design variables have been used to limit the search time of the optimizer. These bounds have been selected based on control engineers' experience and adjusted based on various optimization runs.

As our problem is time dependent and requires response of UAV longitudinal model, therefore, due to the nature of problem, it is not possible to explicitly write our objective and constraints functions. Still, the implicit forms of these are presented below.

III. Formal Problem Statement

Minimize:

$$f(K_1, K_2, K_3) = \int \left(\frac{u_{sim}(t_{new}) - u_{ref}(t_{new})}{\max\limits_{t_{new}} \left| u_{ref} \right|} \right)^2 dt \tag{12}$$

Subject to:

$$
\begin{aligned}
h_1 &= initial\,value + 1 = 0\\
h_2 &= final\,value = 0\\
g_1 &= rise\,time - 2.75 \le 0\\
g_2 &= settling\,time - 7.5 \le 0\\
g_3 &= inital\,undershoot - 0.15 \le 0\\
g_4 &= final\,undershoot - 0.10 \le 0\\
g_5 &= overshoot\,amplitude - 0.15 \le 0\\
g_6 &= |settling\,amplitude| - 0.015 \le 0
\end{aligned}
$$

where

$$
\begin{aligned}
-10 &\le K_1 \le 10\\
-10 &\le K_2 \le 10\\
-100 &\le K_3 \le 10
\end{aligned}
$$

IV. Methodology

The AeroSim Aeronautical Simulation blockset [22] for MATLAB/Simulink was used to incorporate a 6-Degree-of-Freedom (6-DoF) dynamic model of a fixed-wing UAV. This non-linear model includes aerodynamic, propulsion, atmospheric, inertial, Earth and 6-DOF equation of motion in body-axis. Autonomous autopilot and navigation scheme for Aerosonde UAV using AeroSim blockset was accomplished in our previous work [21].

Simulink Design Optimization (SDO) toolbox in conjunction with MATLAB Optimization and Global Optimization toolboxes has been used to minimize the objective function. SDO provides Signal Constraint Block (SCB) to implement the reference signal, constraints, design variables and design variable bounds. SCB, by default provides options to select gradient-based optimization method (*fmincon*) to minimize the objective function. However, if the Global Optimization toolbox is installed then Pattern Search (GA, NM and LH etc.) and Simplex methods are also available as choices.

Now, the desired reference signal (u_{ref}) and constraints implemented in the Simulink Signal Constraint Block appear in Fig. 3. The white area in this figure shows the feasible region for our problem.

We expected objective function to be smooth with only one minimum. Therefore, initially the SQP (*fmincon*) was used to find the optimal solution (x*). However, during the optimization it was discovered that the objective function is non-smooth and multimodal, which will be discussed in next section. Therefore, global method (Genetic Algorithm) was then used. Finally various x^o were used to ensure that we have found the actual and consistent x*.

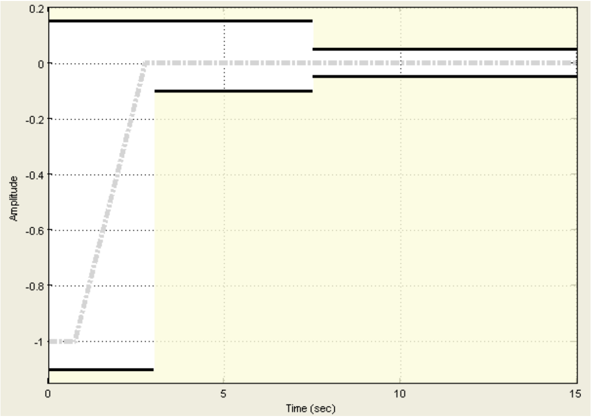

Fig. 3 u_{ref} and Constraints in Simulink SCB

The SCB uses numerical gradients with two options, Basic and Refined. Although our objective function does not have explicit form and hence analytic derivatives cannot be formed, however, SCB does not provide option for analytic gradients anyway.

Tolerance value of $1x10^{-6}$ has been used for constraints, function and parameter values. Moreover, the design variables are gains and do not have any units.

V. Results & Discussions

As stated above, various runs were initially conducted using gradient-based method (*fmincon*) with different initial design values. Out of these, 3 results are presented in Table I. It is found that *fmincon* converges to different x* without finding the global minimum except for one run. In some cases of x^o SCB reports derivative being *NaN* or *Inf* and quits optimization. These results confirm that our objective function is multimodal with various local minima and discontinuous.

TABLE I
Minimization Results with *fmincon*

	RUN 1	RUN 2	RUN 3
x^o	$\{0\ 0\ 0\}$	$\{10\ 10\ 10\}$	$-\{10\ 10\ 10\}$
# of Iter	8	2	3
f_n evals	137	4	5
x*	$\begin{Bmatrix}4.6833\\-1.1001\\-34.2104\end{Bmatrix}$	$\begin{Bmatrix}10\\9.9705\\43.210\end{Bmatrix}$	$\begin{Bmatrix}-10\\-10\\-10\end{Bmatrix}$
f(x)*	0.0182	32.6722	120.06
max g(x)*	0	711	1692
1st-order Optimality	0	0	0

The first-order optimality reported zero in all cases meaning the solution is at minimum but it does not guarantee a global minimum [22]. Graphical representations of these three runs have been shown in appendix A to this paper. Subsequently, Pattern Search with GA search option was used to find the global minimum. The optimization routine found the minima successfully but took large number of iterations and function evaluations. Using x^o of Run 2 and 3, of Table I, following results were found (results for other x^o not shown)

TABLE II
MINIMIZATION RESULTS WITH GENETIC ALGORITHM

Pattern Search (GA)	RUN 1	RUN 2
x^o	$\{10\ \ 10\ \ 10\}$	$-\{10\,10\,10\}$
Iterations for FS	3	13
Func Eval for FS	53	100
Iterations for x^*	101	98
Func Eval for x^*	988	954
x^*	$\begin{Bmatrix} 4.6877 \\ -1.0603 \\ -34.3582 \end{Bmatrix}$	$\begin{Bmatrix} 4.5235 \\ -1.1726 \\ -34.3210 \end{Bmatrix}$
f(x)*	0.0182	0.0183

This demonstrates that cost for finding x* with global method is very high, especially to achieve same level of accuracy as with *fmincon*. Therefore best methodology could be to move to feasible region with any global optimization method and then find the minimum with *fmincon* (if feasible region has only one minimum, which is the case in our function). Table III shows this approach and considerable reduction in overall cost.

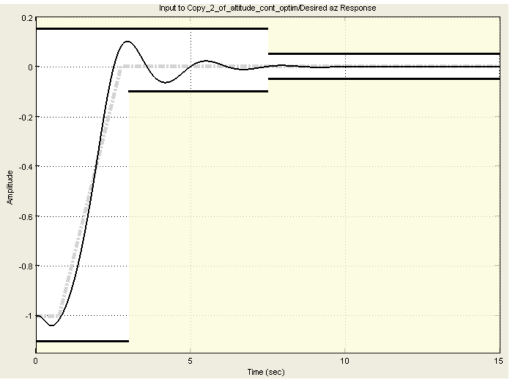

Fig. 4 Pre-Optimization Response

TABLE III
HYBRID APPROACH RESULTS

	RUN 1	RUN 2
x^o	$\{10\ \ 10\ \ 10\}$	$-\{10\,10\,10\}$
Iterations for FS (GA)	3	13
Func Eval for FS(GA)	53	100
Iterations for x^* (*fmincon*)	4	12
Func Eval for x^* (*fmincon*)	20	64

VI. CONCLUSION

The best manually tuned function response before running optimization and final optimized results are shown below for comparison. Refer Figs. 4 & 5. The benefit has been two fold; first the Lead Compensator for Altitude Acquire and Hold is reasonably tuned now for desired response and secondly, the overheads associated with methods discussed in Section I would be reduced significantly for future tuning requirements of all lateral and longitudinal PID controllers and compensators of autopilot.

The objective has been optimized successfully with significant improvement. The multimodal and non-smooth nature of function qualified the use of GA as appropriate minimization algorithm. However, the best approach to find optimum solution for such multimodal functions has been demonstrated with hybrid approach i.e. finding feasible solution with any global method and then getting optimum solution with *fmincon*.

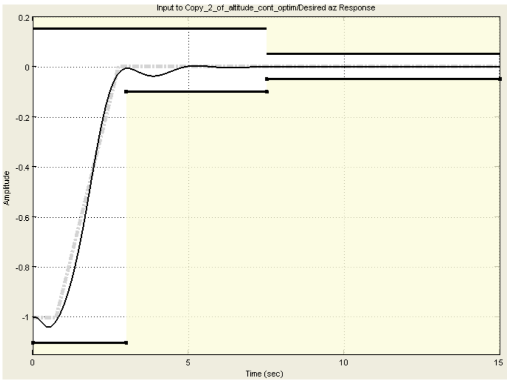

Fig. 5 Optimized Solution

Though Simulink Optimization Toolbox does not provide much flexibility for optimization [1], like analytic gradients for *fmincon* and control over GA configurations (population size, mutation rate etc.) but still it is a good choice to optimize time dependent variables and implicit objective functions.

REFERENCES

[1] Online Documentation and Technical Manuals of Micro-pilot, Piccolo, Athena, & Procerus Autopilot systems.

[2] L. E. Alvarado, "A heading hold PID controller for the TCS L-Band ground targets - Version 2", Project Report System Engineering Directorates. 2008.

[3] J. B. Høstmark, "Modelling simulation and control of fixed-wing UAV: CyberSwan", Master's Thesis, Norwegian University of Science and Technology, 2007.

[4] B. Vanek, J. Bokor, and G. J. Balas, "Longitudinal motion control of a high-speed supercavitation vehicle", Journal of Vibration and Control, 13(2): 159–184, 2007.

[5] M. J. Allen and V. Lin, "Guidance and control of an autonomous soaring UAV", NASA technical report No NASA/TM-2007-214611/REV1, April 2007.

[6] D. Dusha, W. Boles, and Rodney Walker, "Fixed-wing attitude estimation using computer vision based horizon detection". In Proceedings 12th Australian International Aerospace Congress, pp. 1-19, Melbourne Australia, 2007.

[7] A. Chalamont, "Airborne launch and recovery of a UAV to a carrier aircraft", MSc Thesis, Cranfield University, School of Engg, Aerospace Department, Sept 2007.

[8] S. B. Badia, P. Pyk, and P. F. M. J. Verschure, "A fly-locust based neuronal control system applied to an unmanned aerial vehicle: the invertebrate neuronal principles for course stabilization, altitude control and collision avoidance," The International Journal of Robotics Research, Vol. 26, No. 7, July 2007, pp. 759–772.

[9] J. S. Chahl, M. V. Srinivasan, S. W. Zhang, "Landing strategies in honeybees and applications to uninhabited airborne vehicles," The International Journal of Robotics Research, vol. 23,2004, pp. 101.

[10] D. B. Barber, J. D. Redding, T. W. McLain, R. W. Beard, and C. N. Taylor, "Vision-based Target Geo-location using a Fixed-wing

Miniature Air Vehicle," Journal of Intelligent and Robotic Systems, Vol. 47, 2006, pp 361–382.

[11] T. Keviczky and G. J. Balas, "Software-Enabled Receding Horizon Control for Autonomous Unmanned Aerial Vehicle Guidance," Journal of Guidance, Control, and Dynamics, Vol. 29, No. 3, May–June 2006.

[12] S. Sawant, A, Davari, J, Wang, "Trajectory tracking of UAV using robust inventory control techniques," System Theory, 2005. SSST '05. Proceedings of the Thirty-Seventh Southeastern Symposium on, IEEE, 20-22 March 2005.

[13] H. Chao, Y. Cao and Y. Chen, "Autopilots for small unmanned aerial vehicles: a survey", International Journal of Control, Automation, and Systems, 2010, vol. 8, No. 1, pp. 36-44.

[14] M. A. Johnson and M. H. Moradi, PID Control–New Identification and Design Methods, 1st ed., Springer-Verlag, 2005.

[15] H. Grankvist, "Auto pilot design and path planning for a UAV," Scientific Report No. FOI-R-2244-SE, FOI-Swedish Defence Research Agency, Defence and Security, Systems and Technology, Dec 2006.

[16] R. Beard, D. Kingston, M. Quigley, D. Snyder, R. Christiansen, W. Johnson, T, McLain, and M. A. Goodrich, "Autonomous Vehicle Technologies for Small Fixed-Wing UAVs," Journal of Aerospace Computing, Information, and Communication, Vol. 2, January 2005, pp. 92.

[17] P. Kaňovský, L. Smrcek, and C. Goodchild, "Simulation of UAV Systems," Acta Polytechnica, Vol. 45, No. 4, 2005.

[18] S. Puntunan and M. Pamichkun, "Attitude and Heading Control of an Autonomous Flying Robot," The 30th Annual Conference of the IEEE industrial Electronics Society, November 2 - 6, 2004, Busan, Korea.

[19] F. Liang, "Rapid development of UAV autopilot using Matlab/Simulink," AIAA 2002-4976 , AIAA Modeling and Simulation Technologies Conference and Exhibit 5-8 August 2002, Monterey, California, USA.

[20] Matlab, Simulink Design Optimization Users Manual.

[21] M. Ahsan, S. Akhtar, A. Ali, F. Mazhar and M. Khalid, "An Algorithm for Autonomous Aerial Navigation using MATLAB Mapping Toolbox", Proceedings of WASET 2012 , June 27-28, 2012, Paris, France.

[22] Matlab, Optimization Toolbox Users Manual.